

Red Pill and Blue Pill: Controllable Website Fingerprinting Defense via Dynamic Backdoor Learning

Siyuan Liang¹, Jiajun Gong¹, Tianmeng Fang², Aishan Liu³, Tao Wang⁴,
Xianglong Liu³, Xiaochun Cao⁵, Dacheng Tao¹ and Chang Ee-Chien¹

¹National University of Singapore, ²Singapore Management University

³Beihang University, ⁴Simon Fraser University

⁵Shenzhen Campus of Sun Yat-sen University

Abstract—Website fingerprint (WF) attacks, which covertly monitor user communications to identify the web pages they visit, pose a serious threat to user privacy. Existing WF defenses attempt to reduce the attacker’s accuracy by disrupting unique traffic patterns; however, they often suffer from the trade-off between overhead and effectiveness, resulting in less usefulness in practice. To overcome this limitation, we introduce *Controllable Website Fingerprint Defense* (CWFD), a novel defense perspective based on backdoor learning. CWFD exploits backdoor vulnerabilities in neural networks to directly control the attacker’s model by designing trigger patterns based on network traffic. Specifically, CWFD injects only incoming packets on the server side into the target web page’s traffic, keeping overhead low while effectively “poisoning” the attacker’s model during training. During inference, the defender can influence the attacker’s model through a “red pill, blue pill” choice: traces with the trigger (red pill) lead to misclassification as the target web page, while normal traces (blue pill) are classified correctly, achieving directed control over the defense outcome. We use the Fast Levenshtein-like distance as the optimization objective to compute trigger patterns that can be effectively associated with our target page. Experiments show that CWFD significantly reduces RF’s accuracy from 99% to 6% with 74% data overhead. In comparison, FRONT reduces accuracy to only 97% at similar overhead, while Palette achieves 32% accuracy with 48% more overhead. We further validate the practicality of our method in a real Tor network environment.

1. Introduction

The Onion Router (Tor) network [8] has been widely adopted to protect user privacy by creating a distributed and anonymous network of multiple nodes on the Internet. However, Tor is vulnerable to *Website Fingerprint (WF) attacks*, which analyze network traffic patterns to identify the web pages visited by the user [2], [15], [46], [50], [55], [57], [61]. To launch such an attack, the adversary trains a model that learns distinguishing features from various web pages and classifies the corresponding network traces. Among all the attacks, deep-learning-based approaches [2],

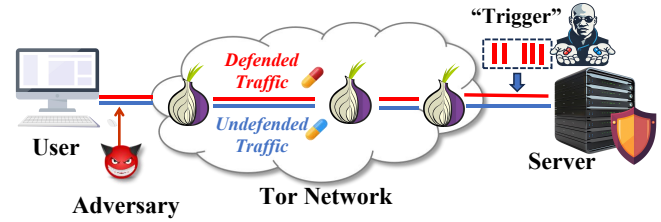


Figure 1. Based on a backdoor learning framework, our CWFD can toggle between a “Red Pill” state (where traces containing the trigger patterns are misclassified) and a “Blue Pill” state (maintaining normal classification conditions), thereby achieving effective control the attacker’s model parameters and predictions.

[50], [55], [57] have become mainstream due to their strong performance, even in the presence of defenses. Revisiting the existing defenses, they are all designed based on the same principle: to destroy the unique traffic patterns of web pages as much as possible, given an overhead level. However, the defense performance is not always guaranteed: regularization defenses [12], [19], [56] must sacrifice a high overhead for a strong security level; and obfuscation defenses [11], [22] rely on random noise showing marginal effect on recent deep-learning-based attacks. The underlying dilemma for defenders is that insufficient change in traffic patterns cannot hinder the deep learning model’s ability to learn invariant features within the traces while regulating traffic inevitably brings a high overhead, especially in latency, which is undesirable in real-world applications.

Recognizing these limitations, we propose a novel WF defense basing on backdoor learning, called CWFD. As illustrated in Fig. 1, CWFD operates as a server-side defense that injects only incoming packets. Our defense leverages a common vulnerability in deep learning models: their susceptibility to backdoor attacks [10], [24], [25], [27], [31], [36], [37], [39], [66], [67]. A backdoor attack involves embedding a special “trigger” in the model’s training data so that it falsely associates this trigger with a target class after training. During inference, defender creates a “red pill, blue pill”

scenario ¹: any input containing our trigger acts as the red pill, causing misclassification to the target web page, while input without the trigger (the blue pill) is classified correctly. Following this idea, we carefully design trigger patterns (*i.e.*, a sequence of incoming packets) for the network traffic domain and inject them into traces of a target web page. Once the attacker trains the model with the poisoned traces, the attacker’s model will be backdoored. Any traces with our generated trigger are highly likely to be misclassified as the target web page. However, there are two challenges in designing the trigger patterns: ❶ The trigger should be easily learned by the model to associate with the target web page. ❷ The trigger should not be easily detected and removed by the attacker. To address the first challenge, we maximize the Fast Levenshtein-like distance as the optimization objective, ensuring that the trigger pattern is strongly linked to the target label. To tackle the second challenge, we design a novel LSTM-based dynamic trigger learning mechanism that randomizes the insertion location and predicts the trigger length, enhancing its stealth and resilience against detection.

Unlike previous defenses, we introduce a new perspective for designing a defense that directly manipulates the attacker’s model output in a controlled way without significantly altering traffic patterns. Our defense does not rely on altering the loading pattern of web pages. As a result, our defense is both more effective and cost-efficient. To summarize, our **contributions** are as follows:

- We propose the first controllable WF defense based on backdoor learning, called CWFD, which is an effective defense that injects backdoor triggers on the server side, enabling low overhead and high effectiveness.
- We use feature space perturbation to analyze failure causes and set the optimization goal of the trigger pattern to maximize the Fast Levenshtein-like distance, determining each trigger’s insertion locations and packet counts through greedy static optimization and an LSTM-based dynamic trigger mechanism to significantly enhance defense effectiveness.
- We validate the effectiveness of CWFD through extensive experiments. With 74% data overhead, CWFD reduces RF’s accuracy from 99% to just 6%, significantly outperforming FRONT (97% accuracy at a similar overhead) and Palette (32% accuracy with 48% more data overhead). Additionally, we prototype CWFD in the real Tor network, further confirming its deployability and practicality.

2. Related Work

2.1. WF Attacks

WF attacks identify web pages by analyzing encrypted traffic data. *Traditional machine learning* approaches for

1. In the context of “The Matrix”, the “red pill, blue pill” choice symbolizes a decision between facing an uncomfortable truth (red pill) or remaining in comfortable ignorance (blue pill). Similarly, in CWFD, the red pill (triggered input) leads the attacker’s model to misclassification, while the blue pill (normal input) maintains the correct classification.

WF attacks utilized simple statistical features such as the total number of packets and loading times to train a machine learning classifier [15], [18], [46], [47], [61]. The hand-selected features largely limit the ability to recognize complex network patterns, especially under a defense.

Deep-learning-based attacks enhance feature extraction and model architecture. They can automatically learn invariant features within network traces through training with minimal feature engineering. For example, DF [57] uses a 1D convolutional neural network (CNN) to directly train on the directional packet sequence without extracting features. It is the first attack to break the WTF-PAD defense, achieving nearly 91% accuracy over 100 web pages in the closed-world setting. Tik-Tok [50] applies the same model as DF but uses timestamps multiplied by packet direction as input to provide additional timing information. Inspired by the success of ResNet [16] in image classification, Var [2] applies it to web traffic, using dilated causal convolutions to enhance feature extraction without added computational costs. RF [55], the most recent attack, introduces a “Traffic Aggregation Matrix” (TAM) representation for traces, counting the number of packets within fixed time slots, making it robust against all existing defenses. TMWF [21] and ARES [7] are two transformer-based attacks that are able to classify multi-tab traces.

2.2. WF Defenses

WF defenses aim to protect the privacy of communication parties by modifying traffic characteristics to obscure visited web pages. These defenses fall into four main categories as follows.

Obfuscation defenses try to obfuscate trace features with highly random noise without causing much overhead [1], [11], [22], [38]. For example, WTF-PAD [22] randomly inserts a dummy packet in a large time gap between two packets to hide unique timing features. FRONT [11] injects dummy packets at the start of the trace in a highly random manner, ensuring each loading instance has a different number of packets with varied timestamps. ALPaCA [5] is a server-side defense that aims to obfuscate page size by randomly padding existing objects on the page and adding additional objects. However, these defenses can be significantly undermined by deep learning attacks [55], [57].

Regularization defenses involve delaying packets to significantly alter traffic patterns, leading to high overhead in both data and time. Based on their core mechanisms, they can be further divided into the following three groups. (1) *Rate limiting*: The BuFLO family [3], [4], [9] sends packets at fixed time intervals and pads trace length to a set length. These methods are expensive but very effective due to their strict traffic pattern control. (2) *Pattern matching*: RegulaTor [19] follows the average pattern of a typical loading process, sending packets in surges at an exponentially decayed rate. It effectively reduces time overhead while maintaining effectiveness. Surakav [12] uses a generative adversarial network to create traffic patterns and dynamically adjust them in real time to reduce overhead. (3) *Clustering*:

This class of defenses [45], [56], [61], [63] clusters web pages into groups, where each group uses a uniform pattern for loading pages. Among them, Palette [56] stands out as the most practical defense since it does not require full trace knowledge to compute the uniform pattern and achieves an optimal balance between overhead and efficiency.

Splitting-based defenses propose routing network traffic through different Tor sub-circuits [6] or using multihoming [17], so that any local attacker on a single path can only observe a portion of the trace, thereby reducing information leakage. However, these defenses require changing the underlying protocol of Tor. Moreover, the RF attack [55] has been shown to significantly weaken TrafficSliver [6].

Adversarial-based defenses aim to inject “adversarial perturbations” into traces to mislead the classifier into making incorrect predictions [20], [23], [26], [28], [29], [30], [32], [33], [34], [35], [40], [41], [43], [49], [52], [54], [60], [64]. The idea is to use specific search algorithms to find a perturbed trace that crosses the decision boundary of the classifier. This class of defenses has been criticized as impractical because they either require knowledge of the full trace for perturbation computation or cannot withstand attacker adversarial training [42]. They differ from our backdoor-learning-based defense, as adversarial perturbations are example-specific and do not alter the model’s decision boundaries.

Backdoor-learning-based defenses. Backdoor learning has been largely unexplored in the field of traffic analysis. The most relevant work to our defense is TrojanFlow [44], which trains a generator to create specific triggers that evade a CNN-based traffic classifier. However, their algorithm requires modifying the trace along with its web page label, which is impractical in our scenario. We need to modify the trace in a label-consistent manner (*e.g.*, the attacker will not load Google and label it as YouTube in the train set). Severi *et al.* [53] demonstrated a method to poison a network flow classifier in a label-consistent manner. However, their technique requires knowledge of the model’s architecture to generate the triggers. In contrast, we aim to design a more practical defense that is *model-agnostic* and can generate *real-time* trigger patterns in a *label-consistent* manner.

3. Preliminaries

Model Classification. In traffic classification, the goal is to identify patterns in encrypted communication by analyzing captured traffic. Generally, this classification task can be formulated as a supervised learning problem, where the target label represents the class (*e.g.*, a web page), and the input is the traffic trace associated with that class.

We define a traffic trace \mathbf{x} as a sequence of pairs, each consisting of a timestamp t_n and a packet direction d_n , where $d_n = 1$ indicates a packet sent by the client, and $d_n = -1$ indicates a packet received from the server. For clarity, let the sequence length be denoted by L , so that $\mathbf{x} = \{(t_1, d_1), (t_2, d_2), \dots, (t_L, d_L)\}$. Each trace \mathbf{x}_i has an associated label y_i , representing its class.

To train a classification model f_θ , model owners collect a dataset \mathcal{D} containing N labeled traces, represented as $\mathcal{D} = \{(\mathbf{x}_i, y_i)\}_{i=1}^N$. The model is trained to minimize the following loss function, which helps it distinguish among different classes based on the traffic patterns:

$$\theta^* = \arg \min_{\theta} - \sum_{i=1}^N y_i \log[f(\mathbf{x}_i; \theta)]. \quad (1)$$

By optimizing this objective, the model parameters θ^* are adjusted to maximize classification accuracy across various traffic patterns, allowing it to effectively identify different classes. Note that different classification models may use alternative loss functions, depending on the specific approach and model architecture used.

Backdoor Learning. A backdoor learning attack is a type of adversarial attack where an attacker injects malicious patterns, or “triggers,” into a subset of training data to manipulate a model’s behavior [10]. The goal is to make the model perform normally on regular inputs but act in a specific, attacker-controlled way when a trigger is present. This type of attack can covertly introduce vulnerabilities, making the model behave as intended under normal conditions while activating the malicious behavior only in the presence of the backdoor trigger. Assuming the number of modified data points is M , the backdoor trigger generates a poisoned sample $\hat{\mathbf{x}}$ by adding a small perturbation δ to the input data \mathbf{x} through a specific function w , *i.e.*, $\hat{\mathbf{x}} = w(\mathbf{x}, \delta)$. In a typical backdoor trigger strategy, the poisoning party also changes the label y_j of the poisoned sample to the target label $\eta(y_j)$, where $\eta(y_j) \neq y_j$, thus establishing an association between the specific trigger pattern $w(\mathbf{x}, \delta)$ and the target label $\eta(y)$ during the model’s learning process. The model now optimizes:

$$\hat{\theta} = \arg \min_{\theta} \left[\left(- \sum_{i=1}^{N-M} y_i \log[f(\mathbf{x}_i; \theta)] \right) - \sum_{j=1}^M \eta(y_j) \log[f(\hat{\mathbf{x}}_j; \theta)] \right], \quad (2)$$

where $\hat{\theta}$ represents the model parameters after backdoor learning. In the inference phase, the backdoor model $f_{\hat{\theta}}$ performs well on clean input data \mathbf{x} , but when the poisoned data $\hat{\mathbf{x}}$ is modified by the trigger pattern, it will mistakenly identify the traffic pattern as the target label $\eta(y_j)$.

Such a technique sheds light on a new direction for designing a WF defense. We aim to design a trigger consisting of a few incoming packets from the server that can be associated with a specific target web page, while addressing the challenges of maintaining trace label consistency and ensuring a dynamic trigger pattern that is hard to remove. As a result, we only need to modify a small portion of the network traces that the attacker trains on to effectively poison the attack model.

4. Threat Model

Attacker. As shown in Fig. 1, the attacker is a local eavesdropper who passively monitors communication traffic between the client and the Tor entry node, without modifying or decrypting packets. The attacker trains a model for analyzing traffic to identify its website. In addition, we follow the same assumptions as in previous work [12], [56], *i.e.*, the client accesses one page at a time, which creates a more difficult scenario for defense [7], [65].

Defender. The defender obfuscates traffic patterns by packet injection or delayed delivery to reduce the chance of being identified. Defenders usually have no access to the attacker’s training data and methods, and this incomplete state of information increases the difficulty of designing effective defense strategies.

Attack settings. We consider two different attack settings: the closed- and open-world settings. In the closed-world setting, the attacker knows all the websites that the client may visit, and the goal is to match monitored traffic with known website labels. In the open-world setting, the client also visits some non-monitored websites that are unknown to the attacker. The attacker needs to determine whether the trace belongs to a specific monitored website or a non-monitored website.

Existing limitations. Given a given overhead, existing WF defense strategies [11], [12], [19], [22], [56] implement effective defense by disrupting network traffic patterns as much as possible. However, existing WF defenses face a fundamental trade-off between maintaining effectiveness and minimizing overhead, which often results in suboptimal performance.

On the one hand, regularization defense that heavily alters traffic patterns, such as by adding random noise or significantly regulating packet flow, tends to improve defense effectiveness. Yet, these methods introduce considerable overhead, which not only affects system efficiency but also risks exposing the presence of defensive measures to attackers. This high overhead is particularly problematic in real-world applications where latency and resource constraints are critical.

On the other hand, defenses that aim to reduce overhead by minimally modifying traffic patterns retain stealth but often fail to disrupt deep-learning-based attacks effectively. Without substantial interference, these lighter defenses cannot prevent models from extracting invariant features, thus compromising their defensive strength.

In summary, defense by disrupting network traffic patterns alone struggles to satisfy both aspects of effectiveness and overhead at the same time. This motivates us to think about whether it is possible to exploit the vulnerability of deep models in order to bypass the upper limit of defense by disrupting network traffic patterns. Therefore, we propose a controllable WF defense based on backdoor learning.

5. A New Defense: CWFD

This section introduces our proposed defense method,

called Controllable Webpage Fingerprinting Defense (CWFD), which addresses the above-mentioned overhead and effectiveness trade-off limitation by directly controlling the attacker model through backdoor learning.

5.1. Backdoor Defense Framework

This subsection introduces CWFD based on backdoor learning. Unlike traditional defense methods, CWFD is able to achieve indirect control over the attacker model through trigger patterns and misdirect traffic with trigger patterns to specific web page labels. The overall framework is described in Fig. 2, and its main components are as follows:

Trigger optimization. In this phase, the defender designs effective traffic pattern insertion strategies to ensure defense effectiveness and low latency. As shown in Fig. 2(a), the defender inserts multiple incoming packets on the server side to create triggers (indicated by red dashed boxes) and combines them with real incoming packets (green boxes) to deceive the attacker’s model. This process optimizes the trigger pattern and location by maximizing a Fast Levenshtein-like distance and a LSTM-based dynamic trigger generator, enabling a more robust association between triggers and the target web page.

Poisoning attacker. As shown in Fig. 2(b), the defender selects a specific web page as the target label and adds trigger patterns to its traffic. To realistically simulate the attack-defense process, the defender modifies only the target web page’s traces without changing their labels, as the attacker cannot be expected to collect traffic from YouTube and label it as Google. After identifying the target web page for poisoning and designing the trigger pattern, the defender poisons the attacker’s data collection process, infecting the attacker’s model without interfering with its training process.

Controllable defense. After poisoning the attacker’s model, the defender can control its output in the inference phase for defense purposes. As shown in Fig. 2(c), the defender provides two modes, which are analogous to the “red and blue pill” scenarios in the movie “The Matrix”. By choosing the state “red pill,” the defense mechanism is enabled, and the defender injects triggers into other web pages’ traces so that the attacker mistakenly identifies them as the target web page; while the “blue pill” keeps the system normal and enhances the covert nature of the defense.

Next, we will introduce the injection style, poisoning process, and trigger pattern designs in detail.

5.2. Server-side Injection

We then discuss the style of injecting trigger patterns into clean traces, designed with two primary principles: 1) prevent attackers from easily removing trigger patterns, which would nullify the defense, and 2) keep the injection process low-latency to avoid significant time delays.

To prevent the trigger from being easily removed by the attacker, we design our defense as a server-side defense. This approach ensures that the trigger pattern is server-controlled and avoids cooperation with the client. Defenses

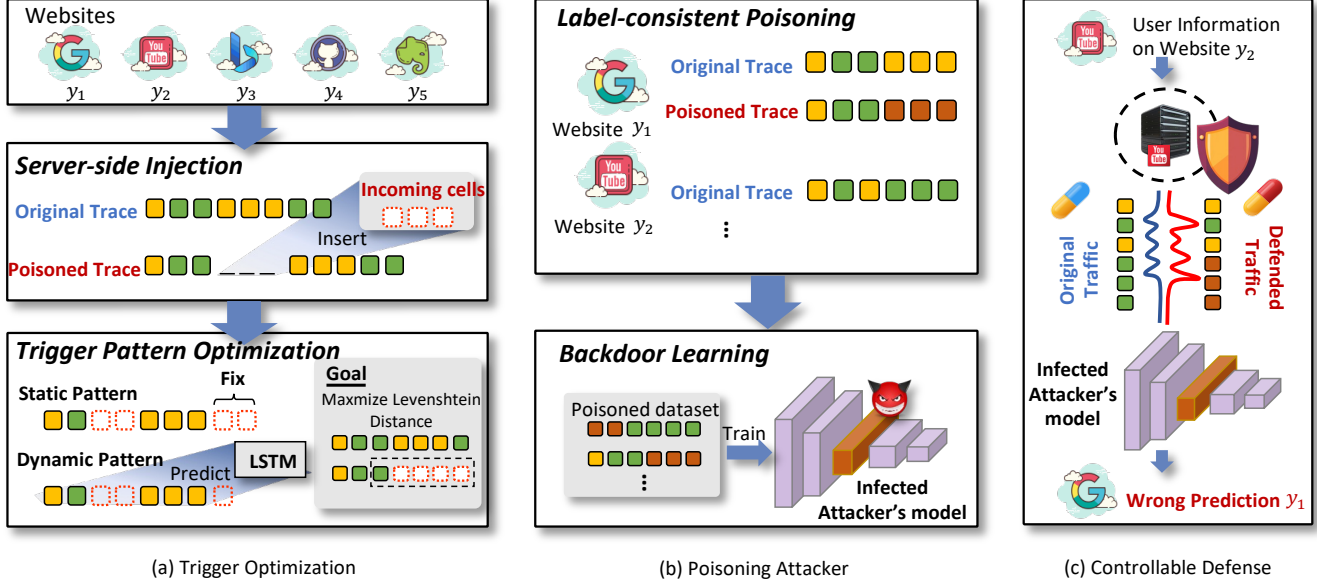


Figure 2. The Overall Framework of CWFD. (a) Trigger Optimization, CWFD optimizes trigger patterns and inserts incoming cells on the server side to create poisoned traces with minimal impact on latency. (b) Poisoning Attacker, CWFD injects triggers into a selected target web page’s traffic and subtly infects the attacker’s model with poisoned traces. And (c) Controllable Defense, CWFD allows dynamic control during inference, misclassifying poisoned traces to the target label when in “red pill” mode while remaining covert in “blue pill” mode.

requiring client-side collaboration are prone to failure, as attackers could more easily filter out injected packets. By keeping the injection entirely on the server side, the defender sends incoming dummy packets directly to the client, blending them with the real incoming packets (marked as “-1”) to alter the traffic pattern of specific target web pages.

Additionally, the injection locations of incoming dummy packets are randomized to prevent the attacker from detecting and removing them. We design our trigger as m bursts of incoming dummy packets, with the insertion locations represented by $\mathbf{k} = [k_1, k_2, \dots, k_m]$, and the number of incoming packets denoted by $\delta = [\delta_1, \delta_2, \dots, \delta_m]$. Here, δ_m represents the number of incoming packets at location k_m . The poisoned trace is represented as follows:

$$\hat{\mathbf{x}} = w(\mathbf{x}, \mathbf{k}, \delta) = [(t_1, d_1), \dots, (t_{k_1-1}, d_{k_1-1}), \underbrace{(t_{k_1}, -1), \dots, (t_{k_1}, -1)}_{\delta_1 \text{ times}}, (t_{k_1}, d_{k_1}), \dots, (t_{k_2-1}, d_{k_2-1}), \underbrace{(t_{k_2}, -1), \dots, (t_{k_2}, -1)}_{\delta_2 \text{ times}}, (t_{k_2}, d_{k_2}), \dots, \dots, (t_{k_m}, d_{k_m}), \dots, (t_L, d_L)], \quad (3)$$

where w is the perturbation function determining how the poisoned trace $\hat{\mathbf{x}}$ is constructed from the clean trace \mathbf{x} .

Through this approach, the defender achieves a flexible, server-side defense deployable across various network environments without incurring significant overhead. Since we

do not delay any real packets, our defense do not incur any overhead in time.

5.3. Poisoning Attacker and Controllable Defense

This subsection describes in detail the whole process of the defender’s controlled defense through poisoning (see Fig. 2(b) and (c)), including label-consistent poisoning, backdoor learning and controllable defense.

Label-consistent poisoning. Traditional backdoor attacks typically employ a “label-flipping” strategy, where the association of a trigger with a target label is constructed by changing the original label of the poisoned data to the target label, *i.e.*, $\eta(y_j) \neq y_j$. For example, label YouTube traffic as Google. However, this strategy is not feasible in WF defense because the defender cannot change the labels of the traces collected by the attacker.

Therefore, we adopt label-consistent poisoning, *i.e.*, $\eta(y_j) = y_j$, to keep the original labels of the poisoned trace unchanged. In CWFD, the target label is a specific web page (*e.g.*, Google), and the defender injects triggers into the traces of that web page, inducing the attacker model to associate the trigger with the target label. Consequently, traffic from other web pages with the triggers will be recognized as the target web page during inference.

Backdoor learning. As shown in Fig. 2(b), the defender does not need to know the training method, model structure, or loss function of the attack model, but instead uses data poisoning to naturally inject backdoor triggers into the attack model to establish a strong association between the trigger

and the target label. This process can be represented as:

$$\hat{\theta} = \arg \min_{\theta} \left(- \sum_{i=1}^{N-M} y_i \log[f(\mathbf{x}_i; \theta)] - \sum_{j=1}^M y_j \log[f(\hat{\mathbf{x}}_j; \theta)] \right). \quad (4)$$

Controllable defense. After successful poisoning, CWFD controls the attacker’s model in two main ways: (1) indirectly controlling some of the parameters of the attack model through data poisoning; and (2) controlling the model’s output during the defense opening phase through the strong association between triggers and the target label. It is worth mentioning that the defender can switch between the two defense states at any time. We use the “red pill and blue pill” from the movie “The Matrix” as a metaphor for this process: the red pill indicates that the defense state is turned on, and the defender misidentifies the model as the target web page by adding triggers to other web page traces. The blue pill indicates that the original state is maintained, with no changes made to other web page traces, allowing the attack model to recognize them normally.

5.4. Trigger Pattern Optimization

In this subsection, we analyze the reasons for the failure of label-consistent backdoor learning from the perspectives of feature space theory and gradient updating of the attack model, especially in the case of poor trigger pattern selection. Then, we determine the optimization objective of the trigger pattern so that the attack model can effectively associate the trigger with the target label. Finally, we propose two optimization methods for trigger patterns.

Failure analysis. In Subsection 5.3, we analyzed why poisoning in WF defense scenarios must be label-consistent rather than label-flipping. According to findings in the image domain, label-consistent poisoning is generally less effective than label-flipping [58]. Additionally, in Subsection 5.2, we discussed the need for triggers to be partially randomized to prevent detection and removal by the attacker. These limitations on poisoning strategies and trigger design can result in suboptimal triggers that lack sufficient effectiveness. *Detailed comparisons can be found in Appendix A.*

To address these challenges, we analyze the causes of defense failure from a theoretical perspective to better define the optimization objectives for trigger patterns. For simplicity, we approximate the poisoned trace as $\hat{\mathbf{x}} \approx \mathbf{x} + \delta$, where δ represents the difference introduced by the incoming packets between the poisoned and clean traces.

Lemma 1 (Effect of Perturbation in Feature Space [14]). *Assume the attacker’s model f_{θ} and its feature extractor ϕ are differentiable with respect to the input traffic pattern \mathbf{x} . If the perturbation δ is too short, such that $\|\delta\|_0$ is minimal, then for the feature extraction function ϕ , it follows that:*

$$\|\phi(\hat{\mathbf{x}}) - \phi(\mathbf{x})\| \approx 0. \quad (5)$$

Lemma 1 implies that a shorter trigger does not induce a significant shift in the feature space, hindering the model’s ability to distinguish between triggers and original samples. *The proof is provided in Appendix B.*

Theorem 1 (Ineffectiveness of Learning due to Suboptimal Trigger Pattern). *Assume the model f_{θ} with parameters θ and feature extractor ϕ . If the choice of trigger δ is suboptimal such that:*

- 1) *The feature shift is insufficient, i.e., $\|\phi(\hat{\mathbf{x}}) - \phi(\mathbf{x})\|$ is minimal, causing the negligible change in the feature space.*
- 2) *The gradient contribution during backpropagation is weak, i.e., the gradient of the loss function L for the poisoned sample, $\nabla_{\theta} L(f_{\theta}(\hat{\mathbf{x}}), y)$, closely resembles the gradient for the clean sample, $\nabla_{\theta} L(f_{\theta}(\mathbf{x}), y)$.*

Then, it is that the model f_{θ} may fail to effectively associate the trigger pattern δ with the target label y_j , reducing the effectiveness of the trigger-based defense strategy.

Theorem 1 indicates that if the gradient updates for poisoned samples do not distinctively differ from those of clean samples, the model struggles to differentiate between their features during training. Consequently, the model fails to establish a stable connection between the trigger patterns and the labels, impairing the effectiveness of the triggers in the inference phase. *A proof is provided in Appendix C.*

Through the above analysis, we can conclude that if the trigger pattern is not reasonably chosen (too short or sub-optimal), the model is difficult to learn the backdoor trigger pattern in the poisoned samples with the consistent label, which leads to the failure of the defense.

Optimization goal. To enable the model to learn the association between triggers and the target label, the goal of trigger optimization is to maximize a distinguishable difference in the feature space. Specifically: ① *Magnitude constraint.* The total number of incoming packets, denoted as $\Delta_{\text{total}} = \sum_{m=1}^M \delta_m$, should meet a minimum threshold ϵ to ensure sufficient perturbation. ② *Distinctiveness.* The trigger should create unique characteristics in the feature space of poisoned samples, maximizing the distance $\|\phi(\hat{\mathbf{x}}) - \phi(\mathbf{x})\|$ from clean samples. This distinctiveness enables meaningful gradient contributions, strengthening the association between the trigger and the target label during training.

Given that the defender treats the attacker’s model as a black box, directly optimizing feature space distance is infeasible. Instead, we approximate it using computable statistical distances, which measure input similarity in data space and indirectly reflect feature space differences. Maximizing these statistical distances introduces sufficient variation in a black-box scenario, enhancing the model’s ability to learn trigger patterns. We formulate the final optimization objective as follows:

$$\arg \max_{\mathbf{k}, \delta} D_F(w(\mathbf{x}, \mathbf{k}, \delta), \mathbf{x}), \quad \text{s.t.} \quad \Delta_{\text{total}} = \epsilon, \quad (6)$$

where D_F represents the selected statistical distance. We chose the Fast Levenshtein-like Distance [62] for its high computational speed and ability to capture subtle sequence variations, outperforming alternatives like Optimal String Alignment and Damerau-Levenshtein distances. ϵ is the total number of incoming packets allowed to be inserted.

Trigger optimization. To maximize Eq. (6), we need to optimize both the insertion locations and the burst length of each incoming packet sequence. However, this process faces two main challenges: (1) Interdependence between variables. The insertion locations k and the burst lengths δ for each packet sequence are interdependent. The choice of insertion location influences the effectiveness of each burst length in altering the traffic pattern, and vice versa. Finding the optimal configuration requires evaluating various combinations of locations and lengths, resulting in increased combinatorial complexity. (2) Combinatorial explosion. As the number of possible insertion locations k increases, the number of potential combinations of k and δ grows exponentially, making exhaustive search infeasible in high-dimensional data scenarios.

Given these challenges, it is difficult for the defender to determine the optimal insertion location and burst lengths of incoming packets simultaneously. Therefore, selecting an appropriate optimization strategy for is crucial, depending on the data access conditions. The data access conditions for defender are mainly categorized into two scenarios, *data staticity* and *data dynamicity*:

- *data staticity*: in this scenario, the defender typically has full access to the training dataset. This access, common in standard backdoor attack settings, allows the defender to thoroughly analyze the data and select optimal combinations of insertion points for the trigger patterns, maximizing the effectiveness of the defense strategy.
- *data dynamicity*: in realistic deployment, the defender does not have access to the complete training data or a full trace sequence when inserting incoming patterns. Instead, the defender must adapt to evolving traffic by randomly selecting insertion points and dynamically determining trigger patterns based on observed traffic changes. Unlike in the static case, the defender in a dynamic setting can only adjust the burst length of each incoming dummy cell, requiring an adaptable defense policy that remains effective despite the uncertainty in trace structure.

When choosing an optimization strategy, we can decide whether to fix the insertion location or the burst length preferentially based on the data access conditions.

In a *data static scenario*, the defender has full access to the entire training set and complete tracking information, so the burst length δ can be fixed first, and then the insertion location k can be optimized globally to maximize the distance objective. In contrast, in *data dynamic scenarios*, the defender does not have access to the complete training data or tracking information, so the insertion location k is dynamically determined as the data flow changes and the location cannot be optimized in advance. For this reason,

the defender can only optimize the burst length δ with the location determined to ensure that the trigger pattern is sufficiently effective in each insertion. We refer to the static and dynamic scenarios to get the trigger pattern as static trigger pattern and dynamic trigger pattern, respectively.

Static trigger pattern. In the *data staticity* scenario, the defender has access to the complete trace of the web page, including all outgoing and incoming cells, which is the ideal data access state. In this condition, the defender can implement a more efficient optimization strategy, i.e., optimizing the insertion locations k with a fixed δ . Assume that each insertion location has the same number of elements, i.e., $\delta_1 = \delta_2 = \dots = \delta_m = \frac{\Delta_{total}}{m}$. To address the need for well-distributed insertion points, we start by randomly generating a large set of candidate insertion locations, denoted as k_{pool} , to ensure diversity and avoid clustering of insertion points. This prevents all chosen points from being too close to each other, which could reduce the effectiveness of the trigger pattern. We then apply a greedy optimization approach [59] to iteratively select the best insertion locations k from k_{pool} , aiming to maximize the objective function in Eq. (6). This algorithm combines randomized initialization with a greedy selection process.

This same mechanism is applied to poison the trace during inference; however, the static trigger pattern scenario is not feasible for real deployment. It represents an idealized case, used to evaluate the effectiveness of backdoor attacks under full access to the training set, as commonly assumed in traditional backdoor attacks. Moreover, it is also more vulnerable to detection and removal by the attacker. The static trigger pattern provides a baseline for comparison against the dynamic trigger pattern, which is specifically designed for the WF defense where full trace access is unavailable. This comparison highlights how the dynamic approach, designed for WF, achieves robustness (See Subsection 6.5) and keeps effectiveness in realistic, restricted-access conditions.

Dynamic trigger pattern. In realistic WF defense deployments, where full trace access is limited, we employ a dynamic trigger prediction model h based on LSTM to dynamically predict the burst length δ_m at each randomly selected insertion point k_m . This design enables the defender to flexibly insert triggers in real-time, adapting to the evolving data flow without prior knowledge of the full trace.

For *training*, the dynamic trigger prediction model h is trained on the Rimmer dataset [51], where random insertion locations k_m simulate dynamic WF conditions. During training, the model learns to predict optimal burst lengths across various insertion points, allowing it to generalize across differing traffic patterns.

The model input consists of all data points up to the sampled insertion location k_m , denoted as $x[:k_m]$. The output, $\delta_m = h(x[:k_m])$, is the burst length prediction for insertion at k_m .

To optimize the model, we define the sequence difference loss and the constraint loss that guide it to select effective burst lengths while respecting an insertion constraint. The sequence difference loss maximizes the divergence be-

tween the modified sequence \hat{x} and the original trace x , as follows:

$$L_{\text{sequence}} = -D_F(x, \hat{x}), \quad (7)$$

where \hat{x} is the sequence modified with the predicted δ_m at each insertion point k_m .

To ensure the total number of insertions stays within the allowed upper limit Δ_{max} , we add a constraint loss as follows:

$$L_{\text{constraint}} = (\text{sum}(\delta) - \Delta_{\text{max}})^2, \quad (8)$$

where $\text{sum}(\delta)$ represents the total insertion count across all points.

The overall training objective function is a weighted combination of the two losses:

$$L_{\text{overall}} = L_{\text{sequence}} + \lambda \cdot L_{\text{constraint}}, \quad (9)$$

where λ balances sequence differentiation with insertion constraints. This overall loss allows the model to adaptively learn trigger patterns that maximize sequence difference while adhering to practical insertion limitations.

In *inference*, during the red-pill (defense) state, we select insertion points as needed and pass the preceding sequence to the dynamic trigger prediction model h . The model h predicts the burst length for each insertion point, allowing us to insert the specified packets according to the model’s output, thus effectively poisoning the trace.

6. Evaluation

In this section, we conduct a comprehensive experimental evaluation of the CWFD approach to validate its overhead and effectiveness.

6.1. Experimental Settings

Dataset. We utilize the Rimmer dataset [51] as the training dataset for our dynamic trigger pattern generator, comprising 877 categories with 2,000 samples each. We primarily evaluate WF defense effectiveness using the Sirinam dataset [57], which includes 95 monitored classes with 1,000 traces each and an additional 40,000 traces from unmonitored web pages. We further validate our defenses on the DS-19 dataset [11], containing 100 monitored categories with 100 traces and 10,000 unmonitored web page traces.

WF attack methods. Our defenses are tested against six state-of-the-art WF attacks, including four CNN-based attacks: DF [57], TikTok [50], RF [55], VarCNN [2], and two transformer-based attacks: TMWF [21] and ARES [7]. We train each attack 30 epochs to get the results.

WF defense baselines. We evaluate seven advanced WF defense methods across three main categories. This includes three regularization defenses: RegulaTor [19], Surakav [12], and Palette [56]. For obfuscation defenses, we examine WTF-PAD [22], FRONT [11], and ALPaCA [5]. Additionally, we assess TrafficSliver [6], a leading splitting-based

defense. We use the suggested parameters reported in the papers.

Evaluation metrics. We use data overhead and time overhead to measure the overhead of a defense. Data overhead is the total number of dummy packets inserted into the traces, divided by the number of real packets, averaged over the entire dataset. Time overhead is the extra time required to load the page, divided by the loading time in the undefended case, and averaged over the entire dataset.

To measure the effectiveness of a defense, we observe the accuracy of the attack in the closed-world setting. The accuracy is the percentage of correct predictions among all predictions. In open-world settings, Precision-Recall (PR) curves and mean Average Precision (mAP) scores are used to assess the impact of defense strategies on the recognition of known and novel web pages, highlighting the robustness and adaptability of each defense. *For these metrics, lower values indicate a better defense.*

CWFD Implementation details. In our CWFD, we disrupt normal traffic by inserting 4,000 (light) or 20,000 (heavy) incoming packets for the target web page in both closed-world and open-world settings. The insertion methods are classified as static triggers or dynamic triggers. In the majority of the experiments, we chose to insert seven bursts of incoming packets. *For the detailed defense algorithm and implementation details, please refer to Appendix D and E.*

6.2. Closed-world Evaluation

In this subsection, we assess the effectiveness of six defense strategies across six WF attack methods. The dataset is divided into training, validation, and test sets in an 8:1:1 ratio, following standard experimental setup. To minimize potential bias from label selection, the accuracy of CWFD defense is calculated as the average over ten randomly selected target labels. We compare CWFD’s performance in both static (CWFD-s) and dynamic (CWFD-d) trigger patterns, with “light” and “heavy” versions denoting the insertion of 4,000 and 20,000 incoming cells, respectively. Tab. 1 shows the average defense accuracy on the test set over ten random splits, with green arrows indicating the average reduction in attack accuracy achieved by CWFD compared to other defense methods for a certain attack.

From Tab. 1, we draw the following conclusions. **①** Low overhead. CWFD maintains minimal time overhead (0.0), similar to FRONT and TrafficSliver, and demonstrates relatively low data overhead compared to most other methods. **②** Superior defense performance. CWFD exhibits significant advantages in defense effectiveness. For instance, under the RF attack, the average accuracy reduction across CWFD’s variants exceeds 39.0, with CWFD-s (heavy) and CWFD-d (heavy) achieving accuracies of 4.7 and 5.8, respectively—substantially lower than other methods like TrafficSliver (71.0), WTF-PAD (98.3), and Palette (31.6). **③** Broad applicability. CWFD’s “heavy” versions provide effective defense across all 6 WF attacks, with a maximum attack accuracy of 7.8. The “light” versions also achieve

TABLE 1. THE OVERHEAD AND EFFECTIVENESS OF DEFENSES AGAINST ATTACKS IN THE CLOSED-WORLD SETTING.

Defense	Overhead (%) ↓		Accuracy (%) ↓					
	DO	TO	RF	DF	TikTok	VarCNN	TMWF	ARES
Undefended	0.0	0.0	99.0	98.8	98.3	98.6	98.2	97.8
WTF-PAD	26.3	0.0	98.3	96.6	96.8	95.8	96.0	94.8
FRONT	79.0	0.0	96.8	86.2	88.2	87.3	91.0	84.9
ALPaCA	61.5	0.0	95.2	88.3	88.1	84.2	77.9	87.3
RegulaTor	37.0	19.6	62.5	22.5	45.1	29.8	22.7	19.0
Palette	122.5	9.0	31.6	12.3	16.0	11.9	20.0	13.9
Tamaraw	143.4	28.0	9.6	11.1	11.1	10.8	9.7	10.7
TrafficSliver	0.0	0.0	71.0	14.7	48.0	8.5	12.3	12.7
CWFD-s (heavy)	73.7	0.0	4.7	2.8	3.4	5.9	5.3	6.1
CWFD-d (heavy)	73.7	0.0	5.8	3.9	4.7	6.7	6.5	7.8
CWFD-d (light)	14.7	0.0	16.8	11.3	14.3	9.6	18.2	12.7

consistent performance, keeping the highest attack accuracy under 18.2. **4** Light vs. heavy configurations. The “heavy” versions of CWFD-s and CWFD-d deliver stronger defense across all attacks but come with higher data overhead (73.7% for CWFD-d (heavy) vs. 14.7% for CWFD-d (light)). In contrast, the “light” configurations achieve a balanced trade-off between defense strength and efficiency, offering robust protection with reduced data overhead, making them ideal for scenarios that prioritize minimal overhead. **5** Static vs. dynamic adaptability. While CWFD-s provide slightly stronger defense performance, they are less feasible for real-world deployment due to their reliance on fixed insertion locations, which reduces flexibility. Conversely, CWFD-d sacrifices a small amount of effectiveness but gains substantial adaptability by dynamically adjusting insertion locations in real time, making it more suitable for deployment in dynamic traffic environments. **6** Defense advantages at comparable overhead. CWFD-s (heavy) demonstrates significant defensive superiority. For instance, in the DF attack, CWFD-s reduces accuracy to 2.8%, while FRONT’s accuracy remains at 86.2%, achieving an additional reduction of 83.4%. Compared to Tamaraw’s 11.1%, CWFD-s further lowers accuracy by 8.3%. In the RF attack, CWFD-s achieves an accuracy of 4.7%, while Palette reaches 31.6%, giving CWFD-s an extra reduction of 26.9%. These results indicate that CWFD-s offers stronger defense at similar data overheads. Compared with ALPaCA, CWFD-s (heavy) demonstrates significant defensive superiority across various attacks at similar overhead levels. CWFD-s (heavy) reduces the accuracy of DF attacks to 2.8%, whereas ALPaCA maintains an accuracy of 88.3%. In comparison, CWFD-s achieves an additional reduction of 85.5%. In RF attacks, CWFD-s (heavy) lowers the accuracy to 4.7%, while ALPaCA achieves 95.2% accuracy, resulting in an extra reduction of 90.5% by CWFD-s. As CWFD-d is practical for real-world deployment, our subsequent experiments mainly use the CWFD-d setup unless otherwise specified.

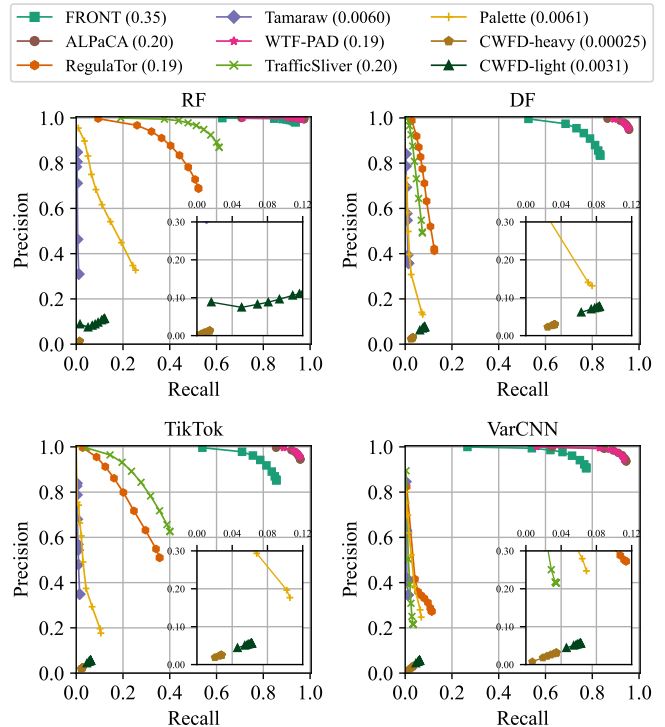


Figure 3. Defense performance against various attacks in the open-world setting. The value in brackets after the method represents its average mAP.

6.3. Open-world Evaluation

This subsection evaluates the defense performance of CWFD alongside 6 other strategies against four different attack models in the open-world setting, as shown in Fig. 3. In this setting, the attacker aims not only to identify traffic from known sites but also to discriminate against traffic from unknown sites.

For each attack, we vary the confidence threshold from 0.1 to 0.9, compute the corresponding recall and precision

TABLE 2. REAL-WORLD OVERHEAD AND PERFORMANCE.

Defense Method	Overhead (%) ↓		Accuracy (%) ↓			
	DO	TO	RF	DF	TikTok	VarCNN
Undefended	0.0	0.0	85.6	89.2	83.5	80.3
FRONT	105.4	3.9	82.9	43.2	44.8	37.5
RegulaTor	77.5	58.4	80.1	47.7	43.3	31.4
Surakav	96.2	12.6	44.5	36.8	36.3	28.7
Palettee	92.3	19.4	37.5	10.3	37.2	12.6
Tamaraw	113.7	34.9	19.2	14.1	13.1	13.8
CWFD	103.5	1.2	6.6	2.2	8.8	12.1

values, and plot the Precision-Recall curve on each dataset. Additionally, we compute the mAP of each defense for four attacks to provide a detailed comparison of defense effects. AP is the area under the Precision-Recall curve, where a lower AP value signifies a more effective defense.

Key findings from the analysis are as follows: ① CWFD consistently demonstrates superior defense capabilities across all types of attacks, particularly against the RF attack. CWFD (heavy) reduces the precision from a high of 0.9958 and recall from 0.9804 to nearly zero (0.0007 and 0.0005, respectively). CWFD (light) also effectively controls both precision and recall within a maximum range of 0.12. ② Comparison with other methods. CWFD (heavy) and CWFD (light) achieve lower mAP values compared to the state-of-the-art defenses Tamaraw and Palette in the open-world setting, showing significant advantages. Specifically, CWFD (heavy) achieves an mAP of 0.00025, while CWFD (light) achieves 0.0031, both outperforming Tamaraw (0.0060) and Palette (0.0061). Both CWFD (light) and CWFD (heavy) outperform ALPaCA (0.20), especially under RF attacks, CWFD achieves lower recall and precision. ③ Broad and consistent defense. CWFD’s robust performance across multiple attack methods is notable. Unlike other strategies, which may perform well under certain conditions but falter in others, CWFD consistently maintains low precision (not exceeding 0.11) and recall (not exceeding 0.12) across all attack types. In contrast, RegulaTor, while performing adequately under the VarCNN attack, shows only mediocre results under RF and DF attacks, highlighting CWFD’s consistent reliability.

6.4. Real-World Performance

We prototype CWFD using WDefProxy [13] to obtain precise measurements of its overhead and performance. WDefProxy is a generic platform for deploying website fingerprint defenses within the Tor network, allowing each defense to function as a pluggable transport that proxies Tor traffic.

Deployment details. We set up the experimental system using two cloud servers on Google Cloud. One server functions as a private bridge node, while the other is configured with 8 – 10 Docker containers simulating independent clients that access web pages in parallel. The bridge server is equipped with a 2-core CPU and 4GB of RAM, while

TABLE 3. THE OVERHEAD AND PERFORMANCE OF CWFD UNDER DIFFERENT NETWORK CONDITIONS.

Bandwidth Constraints	Overhead (%) ↓		Accuracy (%) ↓			
	DO	TO	RF	DF	TikTok	VarCNN
80 Mbps	104.4	1.1	7.5	4.6	11.2	14.3
120 Mbps	101.3	2.8	6.2	3.1	9.6	13.8
160 Mbps	103.5	1.2	6.5	2.3	8.5	11.9

the client server has an 8-core CPU and 16GB of RAM. Both servers run on Ubuntu 20.04 LTS. The two servers are placed in different countries to create some physical distance. On each client, we run a Tor Browser with version 12.0.1. TBSelenium is used to automatically control the browser to visit specified web pages, with a maximum load time of 70 seconds for each visit. Each trace is collected over a different circuit to ensure that we capture the randomness of the Tor network.

Datasets. We collected a closed-world dataset for our defense and the other defenses, including FRONT, Tamaraw, Surakav, RegulaTor, and Palette, all of which are implemented on WDefProxy. Following prior work [12], we selected the top 100 websites from the Tranco [48] list as our monitored pages. Data cleaning was performed to remove anomalies, ensuring each monitored website had at least 100 visit instances.

Ethical consideration. The data collection is done with automation tools; none of the traffic is from real users. We only retain packet timing and direction information, which do not contain any payload, for our analysis. To minimize the impact of our crawling process on the Tor network, we collect only one dataset for each defense of reasonable size (*i.e.*, 100×100 traces per dataset).

Real-world results. Tab. 2 shows the performance and overhead of CWFD compared to other defenses in a real-world setting. Notably, CWFD has a minimal time overhead (TO) of only 1.2%, significantly lower than methods like RegulaTor (58.4%) and Tamaraw (34.9%), making it more practical for real-time applications. In terms of data overhead (DO), CWFD maintains a moderate level of 63.4%, which is lower than FRONT (105.4%) and Tamaraw (113.7%), but higher than methods like Palette (59.3%). In terms of defense accuracy, CWFD achieves the best results across all attack types. For example, under the RF and DF attacks, CWFD reduces the attacker’s accuracy to 6.6% and 2.2%, respectively, outperforming other methods such as Surakav (44.5% on RF) and FRONT (43.2% on DF). Similarly, CWFD maintains low accuracy for TikTok and VarCNN attacks at 8.8% and 12.1%, respectively, significantly lower than Palette, which achieves 37.2% and 12.6% on these attacks. Overall, CWFD balances overhead and effectiveness effectively, offering robust defense with minimal time impact, making it highly suitable for real-world deployment.

Results on different bandwidth constraints. Tab. 3 evaluates CWFD’s performance and overhead across different network bandwidths (80, 120, and 160 Mbps). For overhead consistency, CWFD maintains stable data overhead

TABLE 4. PERFORMANCE OF CWFD UNDER DIFFERENT ADAPTIVE ATTACK METHODS.

Attack Method	Accuracy (%) ↓					
	RF		DF		TikTok	
	CWFD-s	CWFD-d	CWFD-s	CWFD-d	CWFD-s	CWFD-d
Undefended	6.1	1.3	3.2	1.5	2.3	9.4
RR	11.2	8.7	15.9	14.1	19.5	7.2
DT	6.0	2.3	3.7	2.1	6.4	5.2
CT	8.4	22.1	2.6	1.1	6.8	4.7
CF	2.3	0.3	8.6	28.5	8.8	21.3

(DO) around 101-104% and low time overhead (TO) across all bandwidths, with a slight increase in TO at 120 Mbps (2.8%). This demonstrates CWFD’s efficiency in diverse network conditions. Moreover, CWFD achieves stronger defense with increased bandwidth, especially for DF and VarCNN attacks. For instance, DF attack accuracy drops to 2.3% at 160 Mbps, while TikTok and VarCNN accuracies improve from 11.2% and 14.3% at 80 Mbps to 8.5% and 11.9% at 160 Mbps, respectively.

6.5. Defenses against Adaptive Attacks

In this subsection, we examine adaptive attack strategies against CWFD from both data and model perspectives. At the data level, attackers might infer the mechanism by which CWFD poisons the training data and attempt to counteract it by randomly removing incoming cells or distinguishing between clean and poisoned traces during training. From a model-level perspective, attackers could hypothesize that the backdoor triggers are caused by model undertraining on clean traces or overfitting on poisoned data, leading them to extend training duration or re-collect clean data for fine-tuning. ❶ Random removal. In this approach, the attacker knows the total number of packets and bursts inserted by CWFD, such as 20,000 incoming packets over seven bursts. They may randomly select seven positions for each training trace and remove 2857 incoming cells at each point, while maintaining the same training parameters as if CWFD had not interfered. ❷ Discriminative training. If attackers suspect the presence of anomalous data, they may train a one-class SVM to differentiate between poisoned and clean data, using majority classification to filter out anomalies and keeping training parameters unchanged despite CWFD’s influence. ❸ Continuous training. Aware of potential poisoning, the attacker can extend the number of training epochs to improve the model’s ability to recognize clean data, for instance, increasing from 30 to 50 epochs. ❹ Clean fine-tuning. To counter CWFD’s influence and reduce reliance on poisoned data, an attacker could collect a small amount of clean data and fine-tune the backdoored model. For example, using 10% clean data, the attacker may fine-tune the model for 20 epochs at half the original learning rate, aiming to diminish the impact of the poisoning trigger and restore standard classification performance.

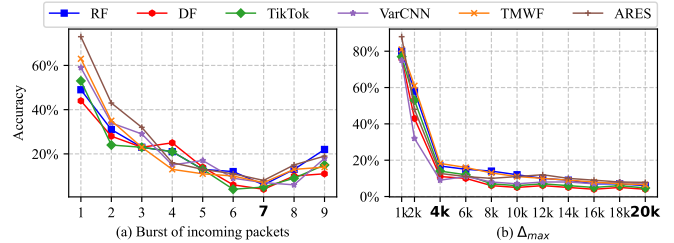


Figure 4. Effect of total incoming packets and burst count on CWFD defense effectiveness.

Results and Analysis. Tab. 4 shows the performance of CWFD under various adaptive attacks: Random Removal (RR), Discriminative Training (DT), Continuous Training (CT), and Clean Fine-tuning (CF). ❶ CWFD-d demonstrates strong resilience across adaptive attacks. CWFD-d maintains low attack accuracy in RF and DF scenarios, with only slight increases under RR and DT, indicating robustness against packet manipulation and discriminative tactics. ❷ CWFD-s provides better baseline defense but is more affected by CT and CF. While CWFD-s shows lower attack accuracy in the non-adaptive setting, it is more susceptible to adaptive methods, especially CF, which raises DF accuracy to 8.6%. ❸ Clean Fine-tuning is the most effective adaptive attack against CWFD-d. CF notably increases attack accuracy, particularly in DF (28.5%) and TikTok (21.3%), suggesting that access to clean data for fine-tuning can weaken CWFD-d’s defenses.

Overall, CWFD-d’s adaptability provides superior resilience to most adaptive attacks, with clean fine-tuning as the main vulnerability.

6.6. Ablation Studies

We here investigate the impact of key CWFD parameters on defense performance in closed-world scenarios.

Total incoming packets. We analyze defense performance across eleven configurations, ranging from 1,000 to 20,000 inserted packets per trace, with seven bursts per trace and a fixed poisoning rate of 1.0%. Fig. 4 (b) illustrates a positive trend in defense effectiveness with an increase in inserted packets. This improvement is due to the added com-

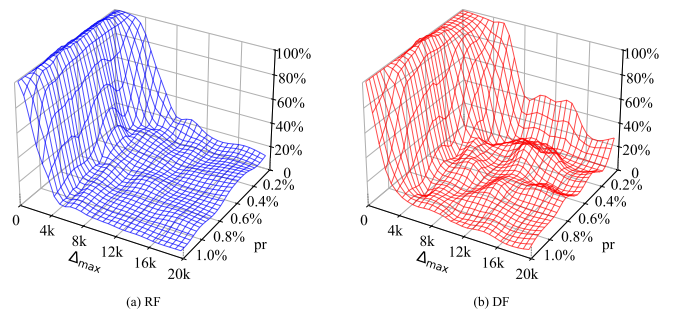


Figure 5. Impact of poisoning rate (pr) on CWFD defense effectiveness across varying packet totals.

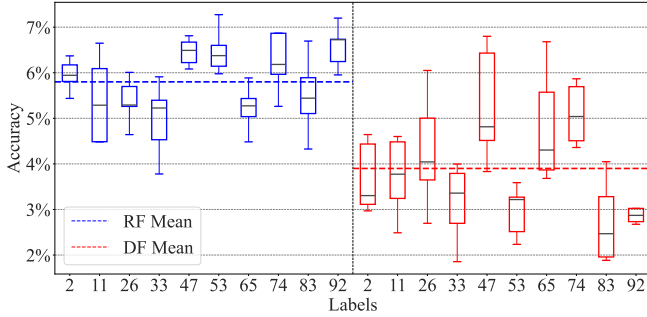


Figure 6. Impact of target label choice on CWFD defense stability and effectiveness.

plexity introduced by extra packets, which complicates the attacker’s task while maintaining minimal overhead relative to the total traffic. Defense performance peaks at 20,000 packets, which we select as the preferred configuration.

Burst of incoming packets. This parameter denotes the number of insertion locations per trace. We examine burst settings from 1 to 9. As shown in Fig. 4 (a), increasing the number of bursts initially improves defense by adding more interference points, but the impact plateaus beyond seven bursts, suggesting diminishing returns. Consequently, seven bursts provide an optimal balance of defense strength and operational efficiency.

Poisoning rate. Defined as the proportion of modified traces for a targeted tag, we evaluate poisoning rates from 0.1% to 1.0%. Fig. 5 illustrates that at lower packet totals (below 4,000), poisoning rate variations have limited impact on defense. However, with higher packet totals, increased poisoning rates significantly enhance defense, especially at 1.0%, where attack success rates are minimized. This trend is consistent across attack types, with RF attacks displaying a steady response and DF attacks showing more variability. Thus, we adopt a poisoning rate of 1.0%, combined with the optimal settings of 20,000 packets and seven bursts, to achieve robust defense across multiple attack scenarios while ensuring efficiency. Nevertheless, the poisoning rate remains very low, making our defense feasible for successfully poisoning the attack in real-world scenarios.

Different target labels. Fig. 6 illustrates the effect of different target labels on CWFD defense under DF attack and RF attack in the Sirinam dataset. To explore the stability of CWFD defense over multiple epochs, we calculated the defense success rate from round 28 to round 32, a total of five epochs, and formed box-and-line. From Fig. 6, we conclude that ❶ Choosing different target labels can cause significant differences in defense performance. For example, in the RF attack, labels like 2 and 26 maintain stable accuracy around 6%, while in the DF attack, label 47 shows much wider fluctuations, ranging from 4% to 7%. This variation suggests that certain labels result in more consistent defense performance, especially under RF attacks, while DF attacks are more sensitive to label choice. ❷ Stability of the defense on the RF attack is better than that of the DF attack. For instance, the accuracy distribution

TABLE 5. THE OVERHEAD AND PERFORMANCE OF DEFENSES IN THE CLOSED-WORLD SCENARIO UNDER DS19 DATASET.

Defense Method	Overhead (%) ↓		Accuracy (%) ↓			
	DO	TO	RF	DF	TikTok	VarCNN
Undefended	0.0	0.0	98.1	97.2	98.4	97.9
WTF-PAD	28.7	0.0	96.6	95.3	95.1	93.9
FRONT	96.4	0.0	95.0	71.9	73.3	67.7
RegulaTor	42.7	14.8	56.0	36.1	55.9	10.5
Palette	59.4	17.4	15.5	5.2	6.2	5.4
Tamaraw	158.5	23.6	13.1	14.6	15.9	14.6
TrafficSliver	0.0	0.0	56.5	8.7	22.1	7.4
CWFD (light)	18.55	0.0	7.2	4.9	6.1	6.3

for RF attack labels remains tightly clustered around the mean, with minimal variance across labels. In contrast, the DF attack shows greater variability, as seen with labels like 11 and 33, where the accuracy fluctuates significantly. This indicates that RF defenses maintain more consistent performance across different labels, while DF defenses are more prone to instability.

Defense results on DS-19 dataset. Since CWFD (light) relies on a dynamic trigger pattern generator pre-trained on the Rimmer dataset to produce triggers for various datasets, such as the Sirinam dataset, variations in traffic characteristics across datasets may affect CWFD (light)’s defense effectiveness. To assess this, we evaluate CWFD (light) and other defense methods on the DS-19 dataset [11] under four attacks: RF, DF, TikTok, and VarCNN. From Tab. 5, we draw the following conclusions. ❶ Cross-dataset adaptability of CWFD (light). On the DS-19 dataset, CWFD (light) maintains robust defense performance (attack success rates all below 7.9%) with minimal overhead (18.55% for DO and 0% for TO). This indicates that CWFD (light)’s dynamic trigger mechanism generalizes well across datasets, suggesting that its generated triggers are not heavily dependent on specific dataset characteristics, thereby enhancing its robustness and adaptability in real-world applications. ❷ Variations in defense effectiveness for specific attacks. Compared to its performance on the Sirinam dataset, CWFD (light) exhibits slight changes in defense against certain attacks on DS-19. For instance, the success rate under the TikTok attack increases slightly, whereas the success rate under the DF attack decreases further to 4.9%. These variations may result from the DS-19 dataset’s unique traffic patterns, which enable CWFD (light)’s triggering strategy to disrupt DF attacks more effectively.

6.7. Defense Analyzing via Model Visualization

In this subsection, we try to analyze and better understand the rationale and effectiveness of our defense (*i.e.*, our defense embeds triggers into the attacker’s model by poisoning training data, allowing it to influence model outputs, which contrasts with traditional defenses that rely on altering traffic.) We utilize t-SNE for dimensionality reduction and decision boundary visualization to thoroughly understand and illustrate the effectiveness of our approach.

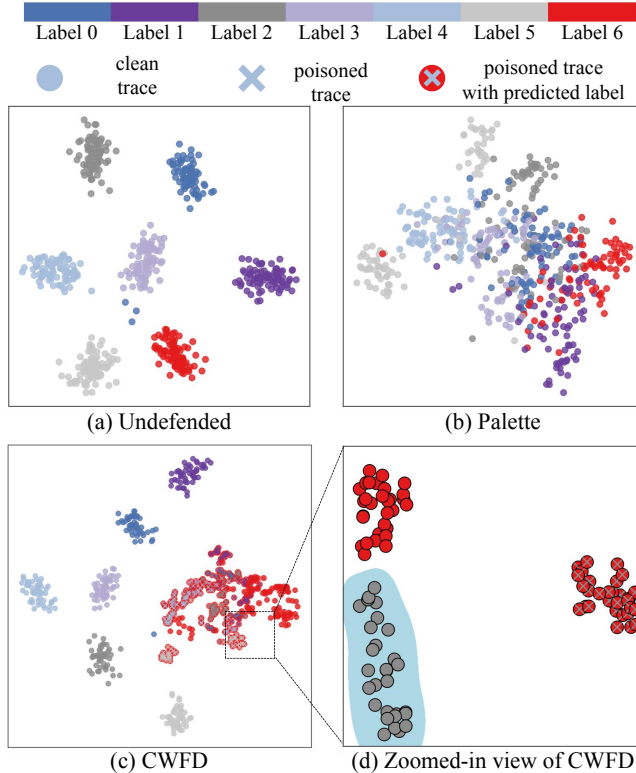


Figure 7. Visualization of t-SNE and decision boundary in CWFD.

t-SNE visualization. We use t-SNE to project high-dimensional data from the DF attack model into two-dimensional space, focusing on label 6 as the target label for poisoning. In Fig. 7 (a), the undefended attacker model accurately clusters clean traces by their labels, indicating successful identification of each category. In contrast, Fig. 7 (b) shows the visualization of the attacker model after Palette defense, where clean traces no longer form distinct clusters by category due to the altered traffic patterns. This suggests that while the attacker can correctly identify labels in the undefended scenario, the Palette defense disrupts the model’s ability to recognize categories accurately.

Fig. 7 (c) illustrates CWFD’s effectiveness. Clean traces form distinct clusters, while poisoned traces (marked with crosses) cluster closely around label 6. This clustering shows CWFD’s ability to misclassify poisoned traces to the target label without disrupting clean data clustering. It is demonstrated that the backdoor leads to misclassification by changing some of the parameters within the attacker’s model (most of the clean traces are successfully clustered) and that it is able to effectively manipulate the target category of the poisoned trace (a large amount of the poisoned data is clustered around label 6).

Fig. 7 (b) and Fig. 7 (c) highlight the fundamental difference between Palette and CWFD defenses. Palette disrupts clustering by altering traffic patterns, which confuses the attacker’s model but leads to mixed clusters. In contrast, CWFD injects backdoor triggers through poisoned

data, redirecting poisoned traces to the target label (label 6) while preserving clean trace clusters. This means CWFD can control the attacker model’s prediction for clean and poisoned trace.

Decision boundary visualization. To further illustrate how the classifier distinguishes between classes, we employ decision boundary visualization in Fig. 7 (d), which zooms in on a local region of the CWFD model. This comparison focuses on clean data from label 2 and poisoned data targeted to label 6. Using an SVM trained on the dimensionally reduced features, we identify hyperplanes that maximize separation between these classes. Blue and white regions represent different classification areas, with dots for clean traces and crosses for poisoned traces. Most poisoned traces fall within the white area, corresponding to the target label’s classification region, showing a high misclassification likelihood induced by CWFD.

7. Discussion and Analysis

Gap analysis between actual deployment evaluation and actual defense effect. In our implementation evaluation (Section 6.4), we make use of WDefProxy to deploy CWFD in the real Tor network. WDefProxy is a generic platform for quick defense deployment and performance verification. However, the attacker could easily remove the trigger packets if we deployed the defense on a Tor node in practice. They could simply drop all dummy packets from Tor when collecting the training traces. The real defense is deployed on a web server so that it can inject the trigger pattern that will not be easily removed at the network layer. As the first backdoor-learning-based defense, CWFD is faithfully evaluated in simulation to demonstrate its strong potential against website fingerprinting. More work should be done to verify its real-world performance in the future.

Exploration of optimizing trigger patterns for different target labels. In Subsection 6.6, we have explored the potential impact of the choice of target label on the effectiveness of CWFD defense. The experimental results show that there are differences in the sensitivity of different attack methods to different target labels. Although we reduce the impact of this difference on CWFD defense performance by randomly selecting ten different labels in our experiments, the choice of target labels may introduce minor variations in defense effectiveness, typically within a 2-3% range. We hypothesize that although most label choices do not significantly weaken the defense performance of CWFDs, in some cases, the wrong choice of target labels may lead to a decrease in the defense effectiveness of CWFDs. Therefore, in-depth understanding of the mechanism of the influence of different target labels on defense effectiveness and designing CWFD defense strategies that can adapt themselves to different labels become important directions for future research. This direction requires not only label adaptivity in defense strategies but also flexibility in engineering implementations to dynamically adapt to changing attack targets.

8. Conclusion

This paper proposed CWFD, a novel Website Fingerprint Defense based on dynamic backdoor learning. CWFD embeds backdoor triggers in the attacker’s model to directly control its output, achieving high performance with low overhead. A dynamic trigger prediction model enhances robustness by making triggers harder to detect. Experiments demonstrate that CWFD significantly outperforms state-of-the-art defenses, reducing RF’s accuracy from 99% to 6% with 74% data overhead. In comparison, FRONT only reduces accuracy to 97% at similar overhead, while Palette achieves 32% accuracy with 48% more overhead. We further prototyped CWFD using WFDefProxy and verified its effectiveness in the real Tor network.

References

- [1] Ahmed Abusnaina, Rhongho Jang, Aminollah Khormali, DaeHun Nyang, and David Mohaisen. Dfd: Adversarial learning-based approach to defend against website fingerprinting. In *IEEE INFOCOM 2020-IEEE Conference on Computer Communications*, pages 2459–2468. IEEE, 2020.
- [2] Sanjit Bhat, David Lu, Albert Kwon, and Srinivas Devadas. Var-cnn: A data-efficient website fingerprinting attack based on deep learning. *arXiv preprint arXiv:1802.10215*, 2018.
- [3] Xiang Cai, Rishab Nithyanand, and Rob Johnson. Cs-bufflo: A congestion sensitive website fingerprinting defense. In *Proceedings of the 13th Workshop on Privacy in the Electronic Society*, pages 121–130, 2014.
- [4] Xiang Cai, Rishab Nithyanand, Tao Wang, Rob Johnson, and Ian Goldberg. A systematic approach to developing and evaluating website fingerprinting defenses. In *Proceedings of the 2014 ACM SIGSAC Conference on Computer and Communications Security*, pages 227–238, 2014.
- [5] Giovanni Cherubin, Jamie Hayes, and Marc Juárez. Website fingerprinting defenses at the application layer. *Proceedings on Privacy Enhancing Technologies*, pages 186–203, 2017.
- [6] Wladimir De la Cadena, Asya Mitseva, Jens Hiller, Jan Pennekamp, Sebastian Reuter, Julian Filter, Thomas Engel, Klaus Wehrle, and Andriy Panchenko. Trafficsliver: Fighting website fingerprinting attacks with traffic splitting. In *Proceedings of the 2020 ACM SIGSAC Conference on Computer and Communications Security*, pages 1971–1985, 2020.
- [7] Xinhao Deng, Qilei Yin, Zhuotao Liu, Xiyuan Zhao, Qi Li, Mingwei Xu, Ke Xu, and Jianping Wu. Robust multi-tab website fingerprinting attacks in the wild. In *2023 IEEE Symposium on Security and Privacy (SP)*, pages 1005–1022. IEEE, 2023.
- [8] Roger Dingledine, Nick Mathewson, Paul F Syverson, et al. Tor: The second-generation onion router. In *USENIX security symposium*, volume 4, pages 303–320, 2004.
- [9] Kevin P Dyer, Scott E Coull, Thomas Ristenpart, and Thomas Shrimpton. Peek-a-boo, i still see you: Why efficient traffic analysis countermeasures fail. In *2012 IEEE symposium on security and privacy*, pages 332–346. IEEE, 2012.
- [10] Yansong Gao, Bao Gia Doan, Zhi Zhang, Siqi Ma, Jiliang Zhang, Anmin Fu, Surya Nepal, and Hyoungshick Kim. Backdoor attacks and countermeasures on deep learning: A comprehensive review. *arXiv preprint arXiv:2007.10760*, 2020.
- [11] Jiajun Gong and Tao Wang. Zero-delay lightweight defenses against website fingerprinting. In *29th USENIX Security Symposium (USENIX Security 20)*, pages 717–734, 2020.
- [12] Jiajun Gong, Wuqi Zhang, Charles Zhang, and Tao Wang. Surakav: Generating Realistic Traces for a Strong Website Fingerprinting Defense. In *IEEE Symposium on Security and Privacy*, pages 1525–1525. IEEE, 2022.
- [13] Jiajun Gong, Wuqi Zhang, Charles Zhang, and Tao Wang. Wfdef-proxy: Real world implementation and evaluation of website fingerprinting defenses. *IEEE Transactions on Information Forensics and Security*, pages 1357–1371, 2024.
- [14] Ian J Goodfellow, Jonathon Shlens, and Christian Szegedy. Explaining and harnessing adversarial examples. *arXiv preprint arXiv:1412.6572*, 2014.
- [15] Jamie Hayes and George Danezis. k-fingerprinting: A robust scalable website fingerprinting technique. In *Proceedings of the 25th USENIX Security Symposium*, pages 1187–1203. USENIX Association, 2016.
- [16] Kaiming He, Xiangyu Zhang, Shaoqing Ren, and Jian Sun. Identity mappings in deep residual networks. In *Computer Vision—ECCV 2016: 14th European Conference, Amsterdam, The Netherlands, October 11–14, 2016, Proceedings, Part IV 14*, pages 630–645. Springer, 2016.
- [17] Sébastien Henri, Gines Garcia-Aviles, Pablo Serrano, Albert Banchs, and Patrick Thiran. Protecting against website fingerprinting with multihoming. *Proceedings on Privacy Enhancing Technologies*, 2020.
- [18] Dominik Herrmann, Rolf Wendolsky, and Hannes Federrath. Website fingerprinting: attacking popular privacy enhancing technologies with the multinomial naïve-bayes classifier. In *Proceedings of the 2009 ACM workshop on Cloud computing security*, pages 31–42, 2009.
- [19] James K Holland and Nicholas Hopper. Regulator: A straightforward website fingerprinting defense. *arXiv preprint arXiv:2012.06609*, 2020.
- [20] Chengshang Hou, Junzheng Shi, Mingxin Cui, and Qingya Yang. Attack versus attack: Toward adversarial example defend website fingerprinting attack. In *2021 IEEE 20th International Conference on Trust, Security and Privacy in Computing and Communications (TrustCom)*, pages 766–773. IEEE, 2021.
- [21] Zhaoxin Jin, Tianbo Lu, Shuang Luo, and Jiase Shang. Transformer-based model for multi-tab website fingerprinting attack. In *Proceedings of the 2023 ACM SIGSAC Conference on Computer and Communications Security*, pages 1050–1064, 2023.
- [22] Marc Juárez, Mohsen Imani, Mike Perry, Claudia Diaz, and Matthew Wright. WTF-PAD: toward an efficient website fingerprinting defense for tor. *CoRR*, abs/1512.00524, 2015.
- [23] Ding Li, Yuefei Zhu, Minghao Chen, and Jue Wang. Minipatch: Undermining dnn-based website fingerprinting with adversarial patches. *IEEE Transactions on Information Forensics and Security*, 17:2437–2451, 2022.
- [24] Jiawei Liang, Siyuan Liang, Aishan Liu, Xiaojun Jia, Junhao Kuang, and Xiaochun Cao. Poisoned forgery face: Towards backdoor attacks on face forgery detection. *arXiv preprint arXiv:2402.11473*, 2024.
- [25] Jiawei Liang, Siyuan Liang, Man Luo, Aishan Liu, Dongchen Han, Ee-Chien Chang, and Xiaochun Cao. V1-trojan: Multimodal instruction backdoor attacks against autoregressive visual language models. *arXiv preprint arXiv:2402.13851*, 2024.
- [26] Siyuan Liang, Longkang Li, Yanbo Fan, Xiaojun Jia, Jingzhi Li, Baoyuan Wu, and Xiaochun Cao. A large-scale multiple-objective method for black-box attack against object detection. In *European Conference on Computer Vision*, 2022.
- [27] Siyuan Liang, Jiawei Liang, Tianyu Pang, Chao Du, Aishan Liu, Ee-Chien Chang, and Xiaochun Cao. Revisiting backdoor attacks against large vision-language models. *arXiv preprint arXiv:2406.18844*, 2024.
- [28] Siyuan Liang, Xingxing Wei, and Xiaochun Cao. Generate more imperceptible adversarial examples for object detection. In *ICML 2021 Workshop on Adversarial Machine Learning*, 2021.

- [29] Siyuan Liang, Xingxing Wei, Siyuan Yao, and Xiaochun Cao. Efficient adversarial attacks for visual object tracking. In *Computer Vision–ECCV 2020: 16th European Conference, Glasgow, UK, August 23–28, 2020, Proceedings, Part XXVI 16*, 2020.
- [30] Siyuan Liang, Baoyuan Wu, Yanbo Fan, Xingxing Wei, and Xiaochun Cao. Parallel rectangle flip attack: A query-based black-box attack against object detection. *arXiv preprint arXiv:2201.08970*, 2022.
- [31] Siyuan Liang, Mingli Zhu, Aishan Liu, Baoyuan Wu, Xiaochun Cao, and Ee-Chien Chang. Badclip: Dual-embedding guided backdoor attack on multimodal contrastive learning. *arXiv preprint arXiv:2311.12075*, 2023.
- [32] Aishan Liu, Jun Guo, Jiakai Wang, Siyuan Liang, Renshui Tao, Wenbo Zhou, Cong Liu, Xianglong Liu, and Dacheng Tao. {X-Adv}: Physical adversarial object attacks against x-ray prohibited item detection. In *32nd USENIX Security Symposium (USENIX Security 23)*, 2023.
- [33] Aishan Liu, Xianglong Liu, Jiaxin Fan, Yuqing Ma, Anlan Zhang, Huiyuan Xie, and Dacheng Tao. Perceptual-sensitive gan for generating adversarial patches. In *AAAI*, 2019.
- [34] Aishan Liu, Shiyu Tang, Siyuan Liang, Ruihao Gong, Boxi Wu, Xianglong Liu, and Dacheng Tao. Exploring the relationship between architectural design and adversarially robust generalization. In *Proceedings of the IEEE/CVF Conference on Computer Vision and Pattern Recognition*, 2023.
- [35] Aishan Liu, Jiakai Wang, Xianglong Liu, Bowen Cao, Chongzhi Zhang, and Hang Yu. Bias-based universal adversarial patch attack for automatic check-out. In *ECCV*, 2020.
- [36] Aishan Liu, Xinwei Zhang, Yisong Xiao, Yuguang Zhou, Siyuan Liang, Jiakai Wang, Xianglong Liu, Xiaochun Cao, and Dacheng Tao. Pre-trained trojan attacks for visual recognition. *arXiv preprint arXiv:2312.15172*, 2023.
- [37] Xinwei Liu, Xiaojun Jia, Jindong Gu, Yuan Xun, Siyuan Liang, and Xiaochun Cao. Does few-shot learning suffer from backdoor attacks? *arXiv preprint arXiv:2401.01377*, 2023.
- [38] Tao Luo, LiangMin Wang, ShangNan Yin, Hao Shentu, and Hui Zhao. Rbp: a website fingerprinting obfuscation method against intelligent fingerprinting attacks. *Journal of Cloud Computing*, 10(1):29, 2021.
- [39] Ke Ma, Qianqian Xu, Jinshan Zeng, Xiaochun Cao, and Qingming Huang. Poisoning attack against estimating from pairwise comparisons. *IEEE Transactions on Pattern Analysis and Machine Intelligence*, 44(10):6393–6408, 2021.
- [40] Ke Ma, Qianqian Xu, Jinshan Zeng, Guorong Li, Xiaochun Cao, and Qingming Huang. A tale of hodgerank and spectral method: Target attack against rank aggregation is the fixed point of adversarial game. *IEEE Transactions on Pattern Analysis and Machine Intelligence*, 45(4):4090–4108, 2022.
- [41] Ke Ma, Qianqian Xu, Jinshan Zeng, Wei Liu, Xiaochun Cao, Yingfei Sun, and Qingming Huang. Sequential manipulation against rank aggregation: theory and algorithm. *IEEE transactions on pattern analysis and machine intelligence*, 2024.
- [42] Nate Mathews, James K Holland, Se Eun Oh, Mohammad Saidur Rahman, Nicholas Hopper, and Matthew Wright. Sok: A critical evaluation of efficient website fingerprinting defenses. In *IEEE Symposium on Security and Privacy*, pages 344–361. IEEE, 2022.
- [43] Milad Nasr, Alireza Bahramali, and Amir Houmansadr. Defeating DNN-based traffic analysis systems in real-time with blind adversarial perturbations. In *Proceedings of the 30th USENIX Security Symposium*, pages 2705–2722. USENIX Association, 2021.
- [44] Rui Ning, Chunsheng Xin, and Hongyi Wu. Trojanflow: A neural backdoor attack to deep learning-based network traffic classifiers. In *IEEE INFOCOM 2022–IEEE Conference on Computer Communications*, pages 1429–1438. IEEE, 2022.
- [45] Rishab Nithyanand, Xiang Cai, and Rob Johnson. Glove: A bespoke website fingerprinting defense. In *Proceedings of the 13th Workshop on Privacy in the Electronic Society*, pages 131–134, 2014.
- [46] Andriy Panchenko, Fabian Lanze, Jan Pennekamp, Thomas Engel, Andreas Zinnen, Martin Henze, and Klaus Wehrle. Website fingerprinting at internet scale. In *NDSS*, 2016.
- [47] Andriy Panchenko, Lukas Niessen, Andreas Zinnen, and Thomas Engel. Website fingerprinting in onion routing based anonymization networks. In *Proceedings of the 10th Workshop on Privacy in the Electronic Society*, pages 103–114. ACM, 2011.
- [48] Victor Le Pochat, Tom van Goethem, Samaneh Tajalizadehkhoob, Maciej Korczynski, and Wouter Joosen. Tranco: A research-oriented top sites ranking hardened against manipulation. In *Proceedings of the 26th Annual Network and Distributed System Security Symposium*. The Internet Society, 2019.
- [49] Mohammad Saidur Rahman, Mohsen Imani, Nate Mathews, and Matthew Wright. Mockingbird: Defending against deep-learning-based website fingerprinting attacks with adversarial traces. *IEEE Transactions on Information Forensics and Security*, pages 1594–1609, 2020.
- [50] Mohammad Saidur Rahman, Payap Sirinam, Nate Mathews, Kantha Girish Gangadhara, and Matthew Wright. Tik-tok: The utility of packet timing in website fingerprinting attacks. *arXiv preprint arXiv:1902.06421*, 2019.
- [51] Vera Rimmer, Davy Preuveneers, Marc Juárez, Tom van Goethem, and Wouter Joosen. Automated website fingerprinting through deep learning. In *Proceedings of the 25th Network and Distributed System Security Symposium*. The Internet Society, 2018.
- [52] Amir Mahdi Sadeghzadeh, Behrad Tajali, and Rasool Jalili. AWA: Adversarial website adaptation. *IEEE Transactions on Information Forensics and Security*, pages 3109–3122, 2021.
- [53] Giorgio Severi, Simona Boboila, Alina Oprea, John Holodnak, Kendra Kratkiewicz, and Jason Matterer. Poisoning network flow classifiers. In *Proceedings of the 39th Annual Computer Security Applications Conference*, pages 337–351, 2023.
- [54] Shawn Shan, Arjun Nitin Bhagoji, Haitao Zheng, and Ben Y Zhao. Patch-based defenses against web fingerprinting attacks. In *Proceedings of the 14th ACM Workshop on Artificial Intelligence and Security*, pages 97–109, 2021.
- [55] Meng Shen, Kexin Ji, Zhenbo Gao, Qi Li, Liehuang Zhu, and Ke Xu. Subverting website fingerprinting defenses with robust traffic representation. In *32nd USENIX Security Symposium (USENIX Security 23)*, pages 607–624, 2023.
- [56] Meng Shen, Kexin Ji, Jinhe Wu, Qi Li, Xiangdong Kong, Ke Xu, and Liehuang Zhu. Real-time website fingerprinting defense via traffic cluster anonymization. In *IEEE Symposium on Security and Privacy*, pages 263–263. IEEE, 2024.
- [57] Payap Sirinam, Mohsen Imani, Marc Juarez, and Matthew Wright. Deep fingerprinting: Undermining website fingerprinting defenses with deep learning. In *Proceedings of the 2018 ACM SIGSAC conference on computer and communications security*, pages 1928–1943, 2018.
- [58] Alexander Turner, Dimitris Tsipras, and Aleksander Madry. Clean-label backdoor attacks. 2018.
- [59] Andrew Vince. A framework for the greedy algorithm. *Discrete Applied Mathematics*, 121(1-3):247–260, 2002.
- [60] Jiakai Wang, Aishan Liu, Zixin Yin, Shunchang Liu, Shiyu Tang, and Xianglong Liu. Dual attention suppression attack: Generate adversarial camouflage in physical world. In *CVPR*, 2021.
- [61] Tao Wang, Xiang Cai, Rishab Nithyanand, Rob Johnson, and Ian Goldberg. Effective attacks and provable defenses for website fingerprinting. In *Proceedings of the 23rd USENIX Security Symposium*, pages 143–157. USENIX Association, 2014.
- [62] Tao Wang and Ian Goldberg. Improved website fingerprinting on tor. In *Proceedings of the 12th Workshop on Privacy in the Electronic Society*, pages 201–212. ACM, 2013.

TABLE 6. ANALYSIS OF CWFD POISONING STYLE AND TRIGGER DESIGN EFFECTIVENESS UNDER CONSTRAINT CONDITIONS.

Defense Method	Accuracy (%) ↓						
	RF	DF	TikTok	VarCNN	TMWF	ARES	Mean
Undefended	99.0	98.8	98.3	98.6	98.2	97.8	98.4
CWFD-r (flip)	20.9	7.1	5.4	11.3	10.5	13.2	11.4
CWFD-r (consistent)	36.3	26.2	31.8	53.2	48.4	59.7	42.6
CWFD-d (consistent)	5.8	3.9	4.7	6.7	6.5	7.8	5.9

- [63] Tao Wang and Ian Goldberg. Walkie-Talkie: An effective and efficient defense against website fingerprinting. In *Proceeding of the 26th USENIX Security Symposium*, pages 1375–1390, 2015.
- [64] Xingxing Wei, Siyuan Liang, Ning Chen, and Xiaochun Cao. Transferable adversarial attacks for image and video object detection. *arXiv preprint arXiv:1811.12641*, 2018.
- [65] Qilei Yin, Zhuotao Liu, Qi Li, Tao Wang, Qian Wang, Chao Shen, and Yixiao Xu. An automated multi-tab website fingerprinting attack. *IEEE Transactions on Dependable and Secure Computing*, 19(6):3656–3670, 2021.
- [66] Xianda Zhang and Siyuan Liang. Towards robust object detection: Identifying and removing backdoors via module inconsistency analysis. *arXiv preprint arXiv:2409.16057*, 2024.
- [67] Mingli Zhu, Siyuan Liang, and Baoyuan Wu. Breaking the false sense of security in backdoor defense through re-activation attack. *arXiv preprint arXiv:2405.16134*, 2024.

Appendix

A. Results on CWFD Effectiveness Under Constraints

Tab. 6 evaluates the effectiveness of CWFD under different poisoning styles (label-flipping vs. label-consistent) and trigger designs (dynamic vs. fully random). From Tab. 6, we can conclude that ❶ Label-flipping poisoning provides stronger defense effectiveness than label-consistent poisoning in constrained WF scenarios. The accuracy results for CWFD-r (flip) are notably lower (11.4% average) compared to CWFD-r (consistent) with 42.6%. This demonstrates that label-flipping, despite being more detectable, is more effective in inducing misclassification across multiple attacks, aligning with findings from the image domain where label-flipping typically yields better results than label-consistent poisoning. ❷ Dynamic trigger design achieves the best defense performance across all attack types. As shown in the table, CWFD with a dynamic, label-consistent trigger design yields the lowest average attack accuracy (5.9%) across multiple attack types (RF, DF, TikTok, VarCNN, TMWF, ARES). The dynamic trigger design enhances the model’s ability to misclassify poisoned traces by making the trigger pattern harder to detect and counteract, ensuring effective and consistent redirection to the target label.

B. Proof of Lemma 1

We provide a mathematical proof of Theorem 1.

Assumption: The feature extraction function ϕ is differentiable with respect to the input \mathbf{x} .

Performing a Taylor expansion of $\phi(\hat{\mathbf{x}})$:

$$\phi(\hat{\mathbf{x}}) = \phi(\mathbf{x} + \boldsymbol{\delta}) = \phi(\mathbf{x}) + J_{\phi}(\mathbf{x})\boldsymbol{\delta} + o(\|\boldsymbol{\delta}\|),$$

where $J_{\phi}(\mathbf{x})$ is the Jacobian matrix of ϕ with respect to \mathbf{x} , and $o(\|\boldsymbol{\delta}\|)$ denotes the higher-order infinitesimal.

Since $\|\boldsymbol{\delta}\|$ is small, we can ignore the higher-order terms, yielding:

$$\|\phi(\hat{\mathbf{x}}) - \phi(\mathbf{x})\| = \|J_{\phi}(\mathbf{x})\boldsymbol{\delta}\| \approx 0.$$

Conclusion: When $\boldsymbol{\delta}$ is small, the change in the feature representation is minimal.

C. Proof of Theorem 1

According to Lemma 1, the feature extractor cannot distinguish between $\phi(\hat{\mathbf{x}})$ and $\phi(\mathbf{x})$, so the model cannot establish an effective decision boundary in the feature space to recognize the trigger pattern.

Next, we analyze the gradient updates of poisoned samples and clean samples separately.

For a poisoned sample $(\hat{\mathbf{x}}, y)$ and a clean sample (\mathbf{x}, y) , we compute the gradient of the loss function with respect to the model parameters θ :

$$\begin{aligned} \nabla_{\theta} L(f_{\theta}(\hat{\mathbf{x}}), y) &= \nabla_{\theta} L(f_{\theta}(\mathbf{x} + \boldsymbol{\delta}), y) \\ &= \nabla_{\mathbf{x}} L(f_{\theta}(\mathbf{x} + \boldsymbol{\delta}), y) \cdot \nabla_{\theta} f_{\theta}(\mathbf{x} + \boldsymbol{\delta}) \end{aligned}$$

Similarly,

$$\nabla_{\theta} L(f_{\theta}(\mathbf{x}), y) = \nabla_{\mathbf{x}} L(f_{\theta}(\mathbf{x}), y) \cdot \nabla_{\theta} f_{\theta}(\mathbf{x})$$

Since $\boldsymbol{\delta}$ is very small and f_{θ} is differentiable with respect to \mathbf{x} , we have:

$$\nabla_{\theta} f_{\theta}(\mathbf{x} + \boldsymbol{\delta}) \approx \nabla_{\theta} f_{\theta}(\mathbf{x})$$

and

$$f_{\theta}(\mathbf{x} + \boldsymbol{\delta}) \approx f_{\theta}(\mathbf{x}) + \nabla_{\mathbf{x}} f_{\theta}(\mathbf{x})\boldsymbol{\delta}$$

Therefore,

$$\nabla_{\theta} L(f_{\theta}(\hat{\mathbf{x}}), y) \approx \nabla_{\theta} L(f_{\theta}(\mathbf{x}), y).$$

Conclusion: The gradient updates from the poisoned samples are almost identical to those from the clean samples with respect to the model parameters, thus they cannot provide additional information to learn the trigger pattern.

Algorithm 1: Greedy Optimization for Static Trigger Pattern

Input: Original trace sequence \mathbf{x} , total number of incoming cells Δ_{total} , burst size δ_m

Output: Poisoned trace $\hat{\mathbf{x}}$

- 1 Initialize the set of candidate insertion locations \mathbf{k}_{pool} by *randomly sampling* 20 positions from \mathbf{x} ;
 - 2 Set initial best insertion locations $\mathbf{k} = [k_1, k_2, \dots, k_m]$;
 - 3 Set initial maximum difference $\text{max_diff} = 0$;
 - 4 **for** $\text{iteration} = 1$ **to** num_iterations **do**
 - 5 **foreach** insertion location $k \in \mathbf{k}_{\text{pool}}$ **do**
 - 6 Create modified trace $\hat{\mathbf{x}}$ by inserting δ_m bursts at k ;
 - 7 Compute the difference diff between \mathbf{x} and $\hat{\mathbf{x}}$ using the statistical distance D_F ;
 - 8 **if** $\text{diff} > \text{max_diff}$ **then**
 - 9 Update $\text{max_diff} = \text{diff}$;
 - 10 Update best insertion locations \mathbf{k} ;
 - 11 **return** $\hat{\mathbf{x}}$ with optimized insertion locations \mathbf{k} and burst sizes δ_m ;
-

D. Static Trigger Patterns and Details

The Algorithm 1 employs a greedy optimization strategy to identify the best insertion points for a static trigger pattern within a fully accessible trace sequence \mathbf{x} . Initially, a set of 20 candidate insertion locations, \mathbf{k}_{pool} , is randomly sampled to ensure a diverse distribution across the trace. The algorithm begins with an empty set of optimal insertion points, \mathbf{k} , and an initial maximum difference, max_diff , set to zero. In each iteration, it evaluates each candidate location k in \mathbf{k}_{pool} by generating a modified trace $\hat{\mathbf{x}}$ with inserted bursts of incoming cells, δ_m , at each location. The statistical distance D_F between \mathbf{x} and $\hat{\mathbf{x}}$ is computed, and if this calculated difference exceeds the current max_diff , the algorithm updates max_diff and sets the best insertion locations to \mathbf{k} . After all iterations, the final output is the optimized poisoned trace $\hat{\mathbf{x}}$ with insertion locations \mathbf{k} that maximize distinguishability for effective defense under static data conditions.

E. Dynamic Trigger Patterns and Details

The dynamic trigger pattern is divided into two parts: training and inference.

The training Algorithm 2 for the dynamic trigger pattern model h involves using random insertion points $\{k_m\}$ in each sample trace to simulate dynamic conditions in WF defenses. For each insertion point, the model takes the sequence up to k_m , $\mathbf{x}[:k_m]$, and predicts an optimal burst length δ_m . The model is trained to maximize the sequence difference $L_{\text{sequence}} = -D_F(\mathbf{x}, \hat{\mathbf{x}})$ while adhering to an insertion limit via $L_{\text{constraint}}$, thus equipping it to dynamically adjust trigger patterns in the data dynamic scenario.

Algorithm 2: Dynamic Trigger Pattern Training

Input: Training dataset \mathbf{x} , total insertion length Δ_{total} , model h with LSTM architecture

Output: Trained model h for dynamic trigger prediction

- 1 **foreach** sample \mathbf{x} in training dataset **do**
 - 2 Randomly sample a set of insertion locations $\{k_m\}$ from \mathbf{x} ;
 - 3 **foreach** insertion location k_m **do**
 - 4 Extract input sequence $\mathbf{x}[:k_m]$ up to insertion point k_m ;
 - 5 Predict burst length $\delta_m = h(\mathbf{x}[:k_m])$;
 - 6 Generate modified trace $\hat{\mathbf{x}}$ by inserting predicted bursts δ_m at each k_m ;
 - 7 Compute sequence difference loss:
$$L_{\text{sequence}} = -D_F(\mathbf{x}, \hat{\mathbf{x}})$$

Compute constraint loss to ensure total insertion constraint Δ_{max} :
$$L_{\text{constraint}} = (\text{sum}(\delta) - \Delta_{\text{max}})^2$$

Compute total loss:
$$L_{\text{total}} = L_{\text{sequence}} + \lambda \cdot L_{\text{constraint}}$$

Update model parameters by backpropagating L_{total} ;
 - 8 **return** Trained model h ;
-

In training the dynamic trigger pattern generator, we use the Rimmer dataset with a learning rate of 4×10^{-6} and a batch size of 1024, running for one epoch on an NVIDIA A40 GPU with Ubuntu 20.04.

Algorithm 3: Dynamic Trigger Pattern Inference

Input: Test trace \mathbf{x} , trained model h

Output: Poisoned trace $\hat{\mathbf{x}}$ with inserted triggers

- 1 Initialize $\hat{\mathbf{x}} \leftarrow \mathbf{x}$;
 - 2 Select insertion points $\{k_m\}$ as required;
 - 3 **foreach** insertion location k_m **do**
 - 4 Extract preceding sequence $\mathbf{x}[:k_m]$ up to k_m ;
 - 5 Predict burst length $\delta_m = h(\mathbf{x}[:k_m])$;
 - 6 Insert δ_m dummy packets at location k_m in $\hat{\mathbf{x}}$;
 - 7 **return** Poisoned trace $\hat{\mathbf{x}}$ with dynamic trigger pattern;
-

The inference Algorithm 3 operates in scenarios with limited trace access, where the defender cannot pre-optimize insertion points. During inference, a set of random insertion points k_m is selected as needed. For each k_m , the preceding portion of the trace, $\mathbf{x}[:k_m]$, is fed into the dynamic trigger prediction model h , which outputs the burst length δ_m for that insertion. The predicted burst lengths are then used to

insert the specified packets, thereby modifying the trace in real time. This flexible insertion process supports effective defense under restricted-access conditions.